

The helicity constraint in turbulent dynamos with shear

Axel Brandenburg^{1,2}, Alberto Bigazzi³, and Kandaswamy Subramanian⁴

¹ *NORDITA, Blegdamsvej 17, DK-2100 Copenhagen Ø, Denmark*

² *Department of Mathematics, University of Newcastle upon Tyne, NE1 7RU, UK*

³ *Department of Mathematics, Politecnico di Milano, Piazza Leonardo da Vinci 32, I-20133 Milano, Italy*

⁴ *National Centre for Radio Astrophysics - TIFR, Poona University Campus, Ganeshkhind, Pune 411 007, India*

2 December 2024

ABSTRACT

The evolution of magnetic fields is studied using simulations of forced helical turbulence with strong imposed shear. After some initial exponential growth, the magnetic field develops a large scale travelling wave pattern. The resulting field structure possesses magnetic helicity, which is conserved in a periodic box by the ideal MHD equations and can hence only change on a resistive timescale. This constrains the growth time of the large scale magnetic field, but only weakly the cycle period. Comparing with the case without shear, the timescale for large scale field amplification is shortened by a factor Q , which depends on the relative importance of shear and helical turbulence, and which controls also the ratio of toroidal to poloidal field. The results are compatible with the idea that α -effect and turbulent magnetic diffusivity of the poloidal field are strongly suppressed by the magnetic field, but that the turbulent diffusivity of the toroidal field is perhaps only weakly affected.

1 INTRODUCTION

In astrophysical bodies such as stars and galaxies there is a strong magnetic field of large scale. Such fields have usually significant magnetic helicity. In the case of the sun significant amounts of magnetic helicity are indeed observed at the solar surface (Berger & Ruzmaikin 2000). However, in unbounded or periodic domains, as well as in perfectly conducting domains, a large scale helical magnetic field can only grow to its final (super-) equipartition field strength on a resistive timescale (Brandenburg 2000, hereafter referred to as B2000). This result is a direct consequence of magnetic helicity conservation which implies that magnetic helicity can only change on a long resistive timescale. The significance of helicity conservation for α -effect mean-field dynamos was first pointed out by Blackman & Field (2000).

An outstanding question is now whether or not this helicity constraint also plays a role in real astrophysical dynamos which differ from those considered in B2000 in several ways: the presence of open boundaries through which magnetic helicity can be lost (both at the surface and at the equator), and the presence of shear through which strong toroidal magnetic fields can be generated without affecting the magnetic helicity.

There is a number of working dynamos which have both open boundaries and shear (e.g., Glatzmaier & Roberts 1995, Brandenburg et al. 1995), but those models are rather complex and use subgrid scale modelling, so one cannot straightforwardly define an effective magnetic Reynolds number. This makes a reliable assessment of the effects of helicity conservation difficult. In order to determine the relative importance of the various possibilities for relaxing the helicity constraint (shear, open boundaries, etc.) it is useful

to consider each possibility in isolation. As a straightforward extension of the model of B2000 we consider here the inclusion of large scale sinusoidal shear, which allows us to retain the assumption of periodic boundary conditions.

We have mentioned already that shear could be important for relaxing the helicity constraint, because the toroidal field generated by stretching does not need to be helical and would hence not be subject to the helicity constraint. On the other hand, shear alone is insufficient for dynamo action: one needs an additional effect that regenerates poloidal (cross-stream) field from toroidal field (e.g. Moffatt 1978, Krause & Rädler 1980). It turns out that it is then no longer the large scale field as such which grows resistively, but rather the *geometrical mean* of the magnitudes of the poloidal and toroidal mean fields. The reason is simple: large scale helicity measures essentially the linkage of poloidal and toroidal fields and must therefore be proportional to the product of the two. This alleviates the resistive constraint somewhat, because now stronger toroidal fields are possible at the expense of weaker poloidal fields or, conversely, equipartition strength large scale fields can be attained in times shorter by the ratio of toroidal to poloidal field strength.

2 THE MODEL

As in B2000 we adopt the MHD equations for an isothermal compressible gas, driven by a given body force \mathbf{f} , which represents both shear and small scale driving;

$$\frac{D \ln \rho}{D t} = -\nabla \cdot \mathbf{u}, \quad (1)$$

$$\frac{D\mathbf{u}}{Dt} = -c_s^2 \nabla \ln \rho + \frac{\mathbf{J} \times \mathbf{B}}{\rho} + \frac{\mu}{\rho} (\nabla^2 \mathbf{u} + \frac{1}{3} \nabla \nabla \cdot \mathbf{u}) + \mathbf{f}, \quad (2)$$

$$\frac{\partial \mathbf{A}}{\partial t} = \mathbf{u} \times \mathbf{B} - \eta \mu_0 \mathbf{J}, \quad (3)$$

where $D/Dt = \partial/\partial t + \mathbf{u} \cdot \nabla$ is the advective derivative, \mathbf{u} is the velocity, ρ is the density, $\mathbf{B} = \nabla \times \mathbf{A}$ is the magnetic field, \mathbf{A} is its vector potential, $\mathbf{J} = \nabla \times \mathbf{B}/\mu_0$ is the current density, η is the magnetic diffusivity, and μ the dynamical viscosity. We adopt a forcing function \mathbf{f} of the form

$$\mathbf{f} = \mathbf{f}_{\text{turb}} + \mathbf{f}_{\text{shear}}, \quad (4)$$

where

$$\mathbf{f}_{\text{shear}} = C_{\text{shear}} \frac{\mu}{\rho} \dot{\mathbf{y}} \sin x \quad (5)$$

balances the viscous stress once a sinusoidal shear flow has been established, and

$$\mathbf{f}_{\text{turb}} = \text{Re}\{N \mathbf{f}_{\mathbf{k}(t)} \exp[i\mathbf{k}(t) \cdot \mathbf{x} + i\phi(t)]\}, \quad (6)$$

is the small scale helical forcing with

$$\mathbf{f}_{\mathbf{k}} = \frac{\mathbf{k} \times (\mathbf{k} \times \hat{\mathbf{e}}) - i|\mathbf{k}|(\mathbf{k} \times \hat{\mathbf{e}})}{2k^2 \sqrt{1 - (\mathbf{k} \cdot \hat{\mathbf{e}})^2/k^2}}, \quad (7)$$

where $\hat{\mathbf{e}}$ is an arbitrary unit vector needed in order to generate a vector $\mathbf{k} \times \hat{\mathbf{e}}$ that is perpendicular to \mathbf{k} , $\phi(t)$ is a random phase, and $N = f_0 c_s (k c_s / \delta t)^{1/2}$, where f_0 is a nondimensional factor, $k = |\mathbf{k}|$, and δt is the length of the timestep. As in B2000 we focus on the case where $|\mathbf{k}|$ is around 5, and select at each timestep randomly one of the 350 possible vectors in $4.5 < |\mathbf{k}| < 5.5$.

We use nondimensional units where $c_s = k_1 = \rho_0 = \mu_0 = 1$. Here, c_s is the sound speed, k_1 is the smallest wavenumber in the box (so its size is 2π), ρ_0 is the mean density (which is conserved), and μ_0 is the vacuum permeability.

We are interested in the case where shear is strong compared with the turbulence, but still subsonic. In B2000 we used $f_0 = 0.1$ and found that the resulting Mach number of the turbulence was between 0.1 and 0.3, which is already too close to one that there would be no room to accommodate sufficiently large shear which is still subsonic. Thus, we now choose f_0 to be ten times smaller, so we take $f_0 = 0.01$. During the saturated phase of the dynamo the resulting rms velocities in the meridional (xz) plane are now around 0.015. For the shear parameter we choose $C_{\text{shear}} = 1$, which leads to toroidal rms velocities of around 0.6, which is about 40 times stronger than the velocities in the meridional plane. We choose a magnetic Prandtl number of ten, i.e. $\mu/(\rho_0 \eta) = 10$, and use $\eta = 5 \times 10^{-4}$, so the magnetic Reynolds numbers based on the box size ($= 2\pi$) for poloidal and toroidal velocities are $R_m^{\text{pol}} = 190$ and $R_m^{\text{tor}} = 7500$, respectively. The poloidal magnetic Reynolds number based on the forcing scale is only about 40, and the kinetic Reynolds number based on the forcing scale is only 4, which is not enough to allow for a proper inertial range. The turnover time based on the forcing scale and the poloidal rms velocity is $\tau = 70$. In the following we denote by poloidal and toroidal components those in the xz -plane and the y -direction, respectively.

As usual for these type of simulations with helical forcing, there is strong dynamo action at small scales amplifying an initially weak random seed magnetic field exponentially (on a dynamical timescale) to equipartition with

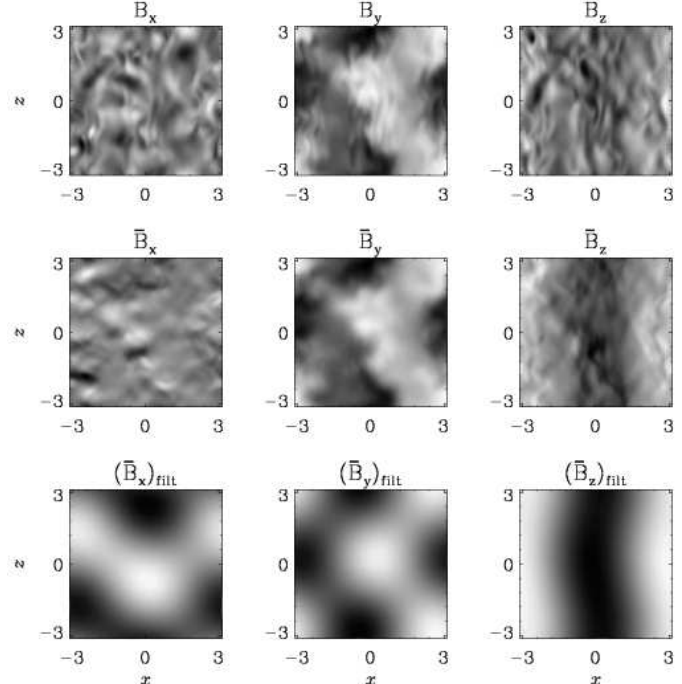


Figure 1. Images of the three components of \mathbf{B} in an arbitrarily chosen xz plane (first row), compared with the y -averaged fields (second row) and the Fourier-filtered y -averaged fields with $|\mathbf{k}| \leq 2$, indicated by the subscript f (third row). 120^3 meshpoints, $t = 6000$.

kinetic energy. The poloidal field, which is strongly dominated by small scales, saturates early on (at $t \approx 1000$) at a level of about 0.010–0.015. The toroidal field saturates later (at $t \approx 2000$) at a level of about 0.2–0.3, and is then already dominated by large scales.

We begin by discussing the resulting field structure at late times, make comparisons with $\alpha\Omega$ dynamo theory and then turn to the question of resistively limited growth of the *large scale* field.

3 FIELD STRUCTURE AND $\alpha\Omega$ DYNAMO

In Fig. 1 we show images of the three field components in the meridional plane. Note that the toroidal field shows much smoother and larger scale structures than the meridional field components. Moreover, the toroidal field shows almost no variation along the y -directions: the toroidal average, \bar{B}_y , (second row), is very similar to an individual meridional cross-section of B_y , first row. However, in contrast to the case without shear, where the mean fields showed systematic variations only in one of the three coordinate directions (B2000), here the toroidal field varies with both x and z , consisting of a superposition of modes with $k_x = 1$ and $k_z = 1$.

The toroidal component of the mean field displays dynamo waves travelling in opposite directions at different x -positions, depending on the local sign of the shear. For $x = -\pi$ the local shear is negative and the dynamo wave travels in the positive z -direction, whilst for $x = 0$ the local shear is positive and the wave travels in the negative

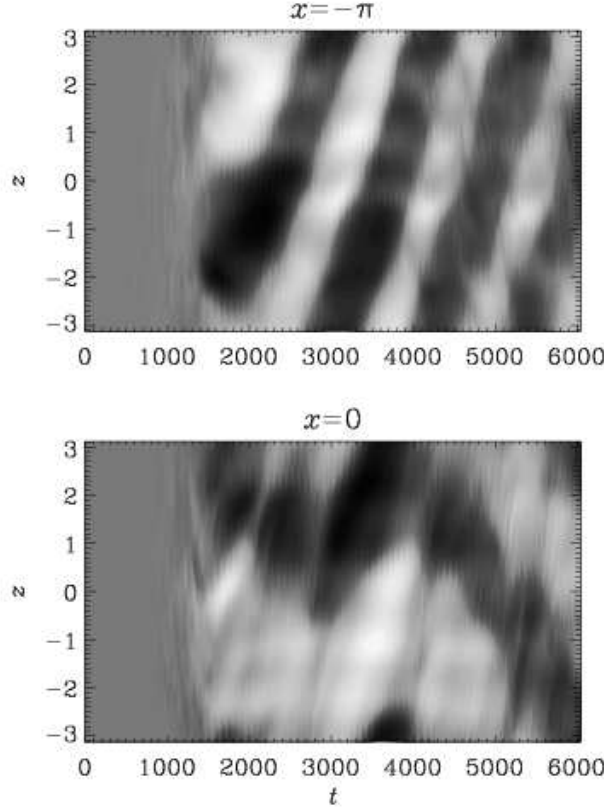


Figure 2. Space-time diagram of the mean toroidal field at $x = -\pi$ (negative local shear) and $x = 0$ (positive local shear). Dark (light) shadings refer to negative (positive) values. Note the presence of dynamo waves travelling in the positive (negative) z -direction for negative (positive) local shear.

z -direction (at least after $t = 4000$); see Fig. 2. This is consistent with what is predicted from mean field $\alpha\Omega$ dynamo theory (e.g. Yoshimura 1975). The behaviour at $x = 0$ is more complicated, suggesting that there is more going on than just two independent dynamo waves.

The results of the simulations without shear were consistent with an α^2 dynamo whose coefficients α and η_T (turbulent diffusivity) were quenched by the magnetic field in similar ways such that the dynamo was just marginally excited. If we assume that the present results (with shear) can also be described by a marginally excited mean-field dynamo we can estimate both α and the total (microscopic plus turbulent) magnetic diffusivity, $\eta_T = \eta + \eta_t$. This was not possible for an α^2 dynamo, but here we have additional information: the cycle period T , which is about 1000 for $x = -\pi$ and about 2000 for $x = 0$. However, unlike the case without shear, the magnetic field is now strongly anisotropic, and it is possible that this field suppresses predominantly the turbulent diffusion of the field in the meridional plane, as it was found numerically by Cattaneo & Vainshtein (1991) using two-dimensional simulations, whilst turbulent diffusion of toroidal field remains strong and is only weakly quenched. This seems plausible, because even a strong toroidal field can be diffused by mutually interchanging toroidal field lines, as was seen in three-dimensional simulations by Nordlund et al. (1994). In the following we take the ratio of the two diffusion coefficients for poloidal and toroidal fields as a free

Table 1. Values of D and C for a marginally excited $\alpha\Omega$ dynamo with given value of ϵ for a one-dimensional and a two-dimensional model.

ϵ	$D_{1\text{-D}}$	$D_{2\text{-D}}$	$C_{1\text{-D}}$	$C_{2\text{-D}}$
1	2	2.4	1	0.57
0.1	0.35	0.4	0.32	0.20

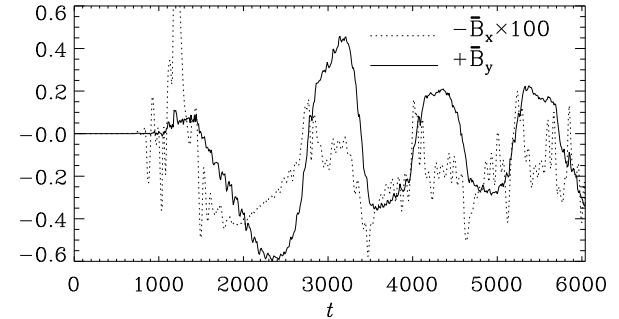


Figure 3. Evolution of $\langle B \rangle_x$ and $\langle B \rangle_y$ at $x = -\pi$ and $z = 0$. Note that $\langle B \rangle_x$ has been scaled by a factor -100 .

parameter ϵ , and assume tentatively $\epsilon \sim 0.1$, which is comparable to the ratio of the velocity dispersion in the poloidal and toroidal directions.

For a linear mean field $\alpha\Omega$ dynamo in a marginally excited state one may define the dynamo number D and the nondimensional cycle frequency C as

$$|\alpha S k_1|/(\eta_T k_1^2) = D, \quad \omega/(\eta_T k_1^2) = C, \quad (8)$$

where $\omega = 2\pi/T$ is the cycle frequency, α is the magnitude of the α -effect, and $S = \partial \bar{u}_y / \partial x$ is the velocity gradient in the x -direction. The parameters D and C depend on ϵ and on details of the model. For a one-dimensional model (ignoring the x -dependence) we have (see appendix A)

$$D = (1 + \epsilon)\epsilon^{1/2}, \quad C = \epsilon^{1/2}. \quad (9)$$

However, a two-dimensional model is more appropriate. We determined numerically the corresponding values of D and C and compare them in Table 1 with those of the one-dimensional model.

Comparing the two-dimensional mean-field model (for $\epsilon = 0.1$, $C = 0.2$, and $D = 0.4$) with the simulations, where $S \approx 0.6$, we find from Eq. (8) that $\eta_T = 0.03$ and $|\alpha| = 7 \times 10^{-4}$ if $T = 1000$, or $\eta_T = 0.016$ and $|\alpha| = 1.6 \times 10^{-4}$ if $T = 2000$ is used. The value of η_T comparable to, or even slightly larger than, the kinematic value, $\tau \langle u_z^2 \rangle \approx 0.013$, which in turn is ~ 30 times larger than the microscopic value, $\eta = 5 \times 10^{-4}$. This is compatible with the idea that, unlike the non-oscillatory α^2 -dynamo of B2000, only the magnetic diffusivity of poloidal field, $\epsilon \eta_T$, is strongly suppressed, but η_T itself is probably not.

There are additional properties of a mean-field dynamo, e.g. the phase shift and amplitude ratio between B_y and B_x , which are also in fair agreement with the simulations: $-B_x$ leads B_y slightly and is several hundred times weaker than

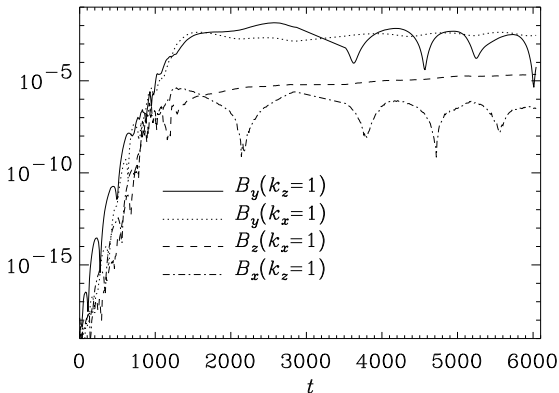


Figure 4. Evolution of the power, $|\hat{B}_i(k_j)|^2$, of a few selected Fourier modes. After $t = 1700$, most of the power is in the mode $|\hat{B}_y(k_z)|^2$, i.e. in the toroidal field component with variation in the z -direction.

B_y ; see Fig. 3. However, the oscillations are markedly non-harmonic, a property which might allow additional information to be gained about the quenching mechanism.

Before we turn to the saturation of the field at the largest scale of the box we first want to assess the relative importance of the different Fourier modes at different times we plot in Fig. 4 the evolution of the power, $|\hat{B}_i(k_j)|^2$, in a few selected modes. Note that after $t = 1700$, most of the power is in the mode $|\hat{B}_y(k_z)|^2$, i.e. the toroidal field component with variation in the z -direction. Between $t = 1700$ until $t \approx 3500$ the ratio of toroidal to poloidal field energies is around 10^4 , so $B_{\text{tor}}/B_{\text{pol}} \approx 100$. At later times this ratio diminishes somewhat. This may suggest that there is a growing contribution from α^2 -type dynamo action. This is also supported by the apparently independent evolution of the oscillatory k_z -mode and the non-oscillatory k_x -mode; see Fig. 4.

In Fig. 5 we show two-dimensional powerspectra of the three components of the mean field, $\overline{\mathbf{B}}$. (Here and elsewhere we denote y -averaged fields by a bar whilst angular brackets are used for full volume averages.) Note that a strong toroidal field builds up first, and at later times the poloidal field components also gain significant power at the largest scale (i.e. at $k^2 < 2$). One should bear in mind, however, that these spectra are for the *mean* fields. The three-dimensional powerspectra of the non-averaged fields reveal that the poloidal fields are ‘noisy’ and possess significant power at the forcing wavenumber, k_f ; see Fig. 6.

The small scale contributions to the poloidal field result from variations in the toroidal direction, as can be seen in a longitudinal cross-section; see Fig. 7, where we show images of the three field components in the yz plane. The figure shows that whilst the toroidal field is relatively coherent in the toroidal direction, the poloidal field components are much less coherent and show significant fluctuations in the y -direction.

We now turn to the temporal evolution of the resulting large scale magnetic field that is gradually emerging in this simulation. We begin by briefly reviewing the main results in the absence of shear (B2000).

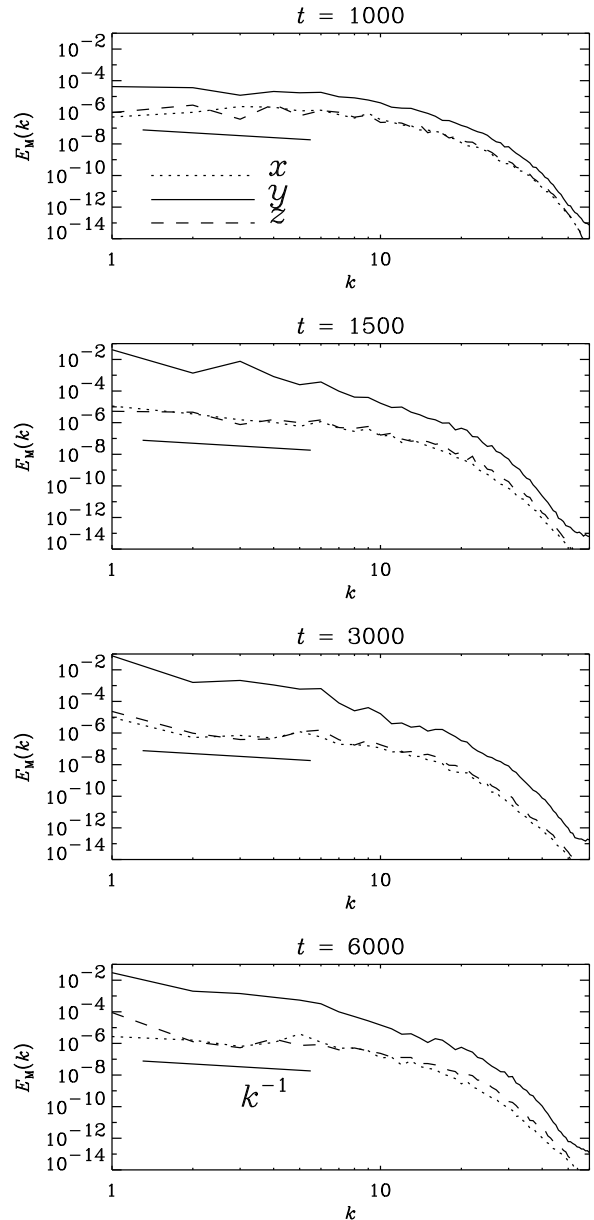


Figure 5. Two-dimensional powerspectra of the three components of the mean field, $\overline{\mathbf{B}}_y$ (solid for the y component, and broken lines for the x and z components. The k^{-1} slope is given for comparison.

4 RESISTIVELY LIMITED GROWTH ON LARGE SCALES

In an unbounded or periodic system the magnetic helicity, $\langle \mathbf{A} \cdot \mathbf{B} \rangle$, can only change if there is microscopic magnetic diffusion, η , and finite current helicity, $\langle \mathbf{J} \cdot \mathbf{B} \rangle$,

$$\frac{d}{dt} \langle \mathbf{A} \cdot \mathbf{B} \rangle = -2\eta \langle \mathbf{J} \cdot \mathbf{B} \rangle. \quad (10)$$

In B2000 a possible configuration for the large scale magnetic field was

$$\overline{\mathbf{B}} = B_0 \begin{pmatrix} \cos(k_1 z + \varphi_x) \\ \sin(k_1 z + \varphi_y) \\ 0 \end{pmatrix}, \quad (11)$$

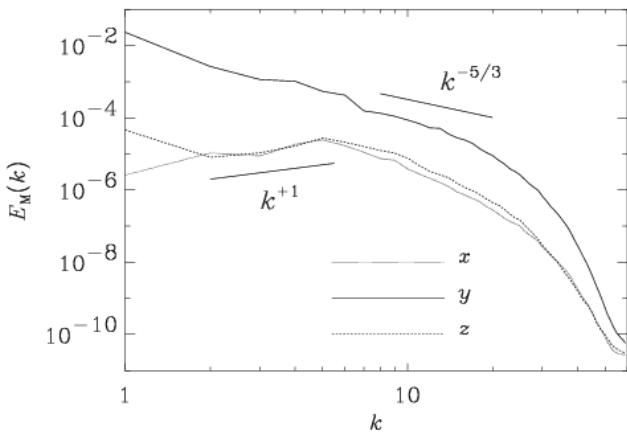


Figure 6. Three-dimensional powerspectrum of the three field components. 120^3 meshpoints, $t = 6000$.

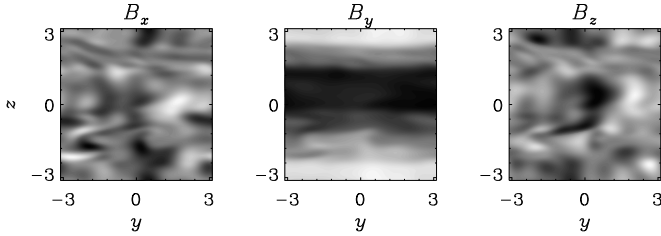


Figure 7. Images of the three components of \mathbf{B} in an arbitrarily chosen yz plane. Note that B_x and B_z show strong variations in y , but B_y does not. $t = 6000$.

which corresponds to a force-free magnetic field that varies in the z -direction, although variations in one of the other two coordinate directions, and with arbitrary phase shifts $\varphi_x \approx \varphi_y$, were also possible (B2000). $B_0 = \langle \bar{\mathbf{B}}^2 \rangle^{1/2}$ is the amplitude, whose time dependence was found to be subject to the helicity constraint (B2000).

The present case differs because of shear which tends to increase the toroidal field, but not the poloidal field. We model this by writing

$$\bar{\mathbf{B}} = \begin{pmatrix} B_{\text{pol}} \cos(k_1 z + \varphi_x) \\ B_{\text{tor}} \sin(k_1 z + \varphi_y) \\ 0 \end{pmatrix}, \quad (12)$$

where B_{pol} and B_{tor} are the amplitudes of the poloidal and toroidal field components. In addition to the z -dependence there can also be an x -dependence of the mean field, which is natural due to the x -dependence of the imposed shear profile. However, for the following argument all we need is the fact that the magnetic and current helicities are proportional to the product of poloidal and toroidal field magnitudes,

$$\langle \bar{\mathbf{J}} \cdot \bar{\mathbf{B}} \rangle / k_1 \approx \mp B_{\text{tor}} B_{\text{pol}} \approx k_1 \langle \bar{\mathbf{A}} \cdot \bar{\mathbf{B}} \rangle, \quad (13)$$

where the upper sign applies to the present case where the kinetic helicity is positive (representative of the southern hemisphere), and the approximation becomes exact if Eq. (12) is valid.

Following B2000, in the steady case $\langle \mathbf{A} \cdot \mathbf{B} \rangle = \text{const}$, see Eq. (10), and so the r.h.s. of Eq. (10) must vanish, i.e.

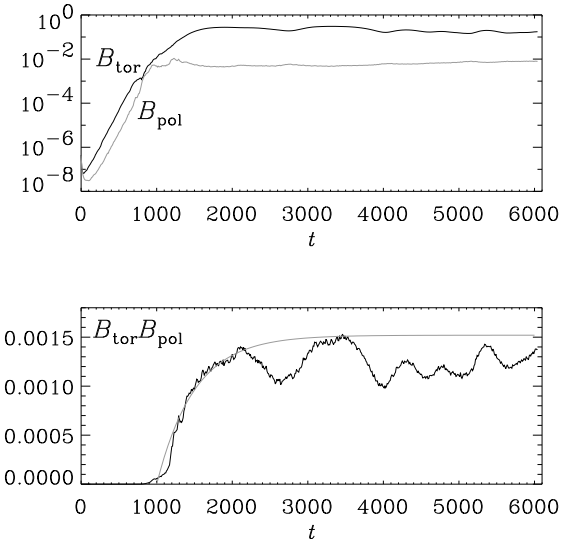


Figure 8. Growth of poloidal and toroidal magnetic fields on a logarithmic scale (upper panel), and product of poloidal and toroidal magnetic fields on a linear scale. For the fit we have used $k_1^2 = 2$ and $\epsilon_0 = 3.8$.

$\langle \mathbf{J} \cdot \mathbf{B} \rangle = 0$, which can only be consistent with Eq. (13) if there is a small scale component, $\langle \mathbf{j} \cdot \mathbf{b} \rangle$, whose sign is opposite to that of $\langle \bar{\mathbf{J}} \cdot \bar{\mathbf{B}} \rangle$. Hence we write

$$\langle \mathbf{J} \cdot \mathbf{B} \rangle = \langle \bar{\mathbf{J}} \cdot \bar{\mathbf{B}} \rangle + \langle \mathbf{j} \cdot \mathbf{b} \rangle \approx 0. \quad (14)$$

This yields, analogously to B2000,

$$-\frac{d}{dt} (B_{\text{tor}} B_{\text{pol}}) = +2\eta k_1^2 (B_{\text{tor}} B_{\text{pol}}) - 2\eta k_1 |\langle \mathbf{j} \cdot \mathbf{b} \rangle|, \quad (15)$$

which yields the solution

$$B_{\text{tor}} B_{\text{pol}} = \epsilon_0 B_{\text{eq}}^2 \left[1 - e^{-2\eta k_1^2 (t - t_s)} \right], \quad (16)$$

where $\epsilon_0 = |\langle \mathbf{j} \cdot \mathbf{b} \rangle| / (k_1 B_{\text{eq}}^2)$ is a prefactor, B_{eq} is the equipartition field strength with $B_{\text{eq}}^2 = \mu_0 \langle \rho u^2 \rangle$, and t_s is the time when the small scale field has saturated which is when Eq. (15) becomes applicable. All this is equivalent to B2000, except that $\langle \bar{\mathbf{B}}^2 \rangle$ is now replaced by the product $B_{\text{tor}} B_{\text{pol}}$. The significance of this expression is that large toroidal fields are now possible if the poloidal field is weak.

In order to compare with the simulation we now define

$$B_{\text{tor}} \equiv \langle \bar{B}_y^2 \rangle^{1/2}, \quad B_{\text{pol}} \equiv \langle \bar{B}_x^2 + \bar{B}_z^2 \rangle^{1/2}, \quad (17)$$

Note that this definition generalizes that given in Eq. (12). In Fig. 8 we show the evolution of B_{tor} and B_{pol} and compare the evolution of the product $B_{\text{tor}} B_{\text{pol}}$ with Eq. (16). There are different stages; for $1200 < t < 2200$ and $3000 < t < 3700$ the effective value of k_1^2 is $k_1^2 = 2$ (because there are contributions from $k_x = 1$ and $k_z = 1$; see Fig. 4), whilst at other times ($2500 < t < 2800$ and $t > 4000$) the contribution from $k_x = 1$ (for $2500 < t < 2800$) or $k_z = 1$ (for $t > 4000$) has become subdominant and we have effectively $k_1^2 = 1$. This is consistent with the change of field structure discussed in the previous section: for $2000 < t < 3000$ and around $t = 4000$ the $B_y(k_x = 1)$ mode is less powerful than the $B_y(k_z = 1)$ mode.

5 TIMESCALE CONSTRAINT FOR THE SUN

The main result of this paper is a quantitative modification of the helicity constraint for dynamos in the presence of shear. With shear included the estimate for $\langle \bar{B}^2 \rangle$ of B2000 is now to be replaced by the product $B_{\text{tor}} B_{\text{pol}} \approx \langle \bar{B}^2 \rangle / Q$, where $Q = B_{\text{tor}} / B_{\text{pol}} \gg 1$ and so $\langle \bar{B}^2 \rangle \approx B_{\text{tor}}^2$. For *early times*, the exponential function in Eq. (16) can be expanded:

$$\langle \bar{B}^2 \rangle \approx \epsilon_0 B_{\text{eq}}^2 2\eta k_1^2 (t - t_s) Q. \quad (18)$$

In the case of efficient large scale dynamo action the small scale current helicity is very nearly equal to the normalized kinetic helicity, $\rho_0 \langle \boldsymbol{\omega} \cdot \mathbf{u} \rangle$ (see also Brandenburg & Subramanian 2000), which in turn is approximately $k_f \langle \rho \mathbf{u}^2 \rangle$. Since $\epsilon_0 = \langle \mathbf{j} \cdot \mathbf{b} \rangle / (k_1 B_{\text{eq}}^2)$, this leads to $\epsilon_0 \approx k_f / k_1$, which is 5 in the present case.

We now want to estimate the time, τ_{eq} , required to build up a large scale field of equipartition field strength, i.e. $\langle \bar{B}^2 \rangle = B_{\text{eq}}^2$. In units of the turnover time, $\tau = L / u_{\text{rms}}$, we have

$$\tau_{\text{eq}} / \tau = u_{\text{rms}} L / (2\eta k_1^2 L^2 \epsilon_0 Q) = R_{\text{m}} / (\epsilon_1 Q), \quad (19)$$

where we have introduced a new coefficient $\epsilon_1 = 2\epsilon_0 k_1^2 L^2$. Applying this to the sun we have $\tau_{\text{eq}} / \tau \approx 10^4 - 10^7$, if we assume $R_{\text{m}} = 10^8 - 10^{10}$, $Q = 10 - 100$, and $\epsilon_1 \approx (2\pi)^2 \approx 100$. The ratio of the solar 22-year magnetic cycle period and the turnover time of about ten days is 800, which is significantly smaller than the ratio predicted by Eq. (19). Thus, even in the presence of shear the helicity constraint could still pose a problem for the sun. On the other hand, it is not clear that the cycle period is strongly effected by the helicity constraint. However, before making more detailed comparisons with the sun it would be important to assess the importance of open boundaries, for example. This seems to be now one of the most important remaining aspects to be clarified in the theory of large scale dynamo; see also Blackman & Field (2000) and Kleeorin et al. (2000). The effects of open boundaries are likely to be especially important in cases with outflows (e.g. in protostellar accretion discs or in active galactic nuclei). It should also be mentioned that dynamos may operate with non-helical flows; see the recent paper by Vishniac & Cho (2000). This may relax the helicity constraint, but so far there are no simulations supporting this possibility.

6 CONCLUSIONS

The present investigations have shown that the effects of the helicity constraint can clearly be identified, even though much of the field amplification results now from the shearing of a poloidal field. Instead of having a constraint on the magnetic energy, one now has a constraint on the geometrical mean of the energies in the poloidal and toroidal mean field components. The dynamo remains time dependent with a typical period $T \approx 1000 \approx 14\tau$. The toroidally averaged field alternates in sign with clear signs of migration. Unlike the case without shear, the turbulent magnetic diffusivity is no longer quenched to its microscopic value.

The present work has also revealed that, even though the kinetic helicity of the flow is near to its maximum possible value, the poloidal field shows a great deal of

‘noise’, whilst the toroidal field does not. Powerspectra of the poloidal field show that most of the power is in small scales, making the use of averages at first glance questionable. However, once the field is averaged over the toroidal direction the resulting poloidal field is governed by large scale patterns (the slope of the spectrum is steeper than k^{-1} , which is the critical slope for equipartition of energy between small and large scale fields). The presence even of a weak poloidal field is crucial for understanding the resulting large scale field generation in the framework of an $\alpha\Omega$ dynamo.

The results of the simulations can possibly be reproduced by a mean-field model where the alpha-effect and the turbulent magnetic diffusivity of the poloidal field are strongly quenched by the magnetic field, but the turbulent magnetic diffusivity of the toroidal field is quenched only weakly. This would imply that the cycle period has a weaker dependence on the magnetic Reynolds number than the growth time of the dynamo.

ACKNOWLEDGMENTS

We thank Anvar Shukurov for many stimulating discussions and comments on the manuscript. ABi and KS acknowledge Nordita for hospitality during the course of this work. Use of the PPARC supported supercomputers in St Andrews and Leicester is acknowledged.

REFERENCES

Berger M. A. & Ruzmaikin A. 2000, JGR 105, 10481
 Blackman E. G. & Field G. F. 2000, ApJ 534, 984
 Brandenburg A. 2000, ApJ, astro-ph/0006186 (B2000)
 Brandenburg A. & Subramanian K. 2000, A&A 361, L33
 Brandenburg A., Nordlund Å., Stein R. F. & Torkelsson U. 1995, ApJ 446, 741
 Cattaneo, F. & Vainshtein, S. I. 1991, ApJ (Letters) 376, L21
 Glatzmaier G. A. & Roberts P. H. 1995, Nat 377, 203
 Kitchatinov L. L., Rüdiger G. & Pipin V. V. 1994, Astr. Nachr. 315, 157
 Kleeorin N. I., Moss D., Rogachevskii I. & Sokoloff D. 2000, A&A 361, L5
 Krause F. & Rädler K.-H. 1980, Mean-Field Magnetohydrodynamics and Dynamo Theory (Pergamon Press, Oxford)
 Moffatt H. K. 1978, Magnetic Field Generation in Electrically Conducting Fluids (CUP, Cambridge)
 Nordlund, Å., Galsgaard, K. & Stein, R. F. 1994, in Solar surface magnetic fields, ed. R. J. Rutten & C. J. Schrijver (NATO ASI Series, Vol. 433), p.471
 Pouquet A., Frisch U. & Léorat J. 1976, JFM 77, 321
 Vishniac E. T. & Cho J. 2000, ApJ, astro-ph/0010373
 Yoshimura H. 1975, ApJ 201, 740

APPENDIX A: MEAN-FIELD MODEL WITH ANISOTROPIC MAGNETIC DIFFUSIVITY

We present here the calculation of the dependencies (9) for the simple one-dimensional mean-field model with anisotropic magnetic diffusivity. Assuming that α and η_T are constant, and that the magnetic diffusion of poloidal field is smaller than that of the toroidal field by a fraction ϵ , the $\alpha\Omega$ dynamo equations can be written in the form

$$\dot{\overline{B}}_x = -\alpha \overline{B}'_y + \epsilon \eta_T \overline{B}''_x, \quad (A1)$$

$$\dot{\overline{B}}_y = S \overline{B}_x + \eta_T \overline{B}''_y, \quad (A2)$$

where primes and dots denote z - and t -derivatives, respectively. The dispersion relation is

$$(\lambda + \eta_T k^2)(\lambda + \epsilon \eta_T k^2) + ik\alpha S = 0. \quad (A3)$$

For the marginally excited state, $\lambda = -i\omega$, we have

$$-\omega^2 - i\omega(1 + \epsilon)\eta_T k^2 + \epsilon(\eta_T k^2)^2 + ik\alpha S = 0, \quad (A4)$$

where all quantities are real. Thus, we have two equations,

$$-\omega^2 + \epsilon(\eta_T k^2)^2 = 0, \quad (A5)$$

and

$$-\omega(1 + \epsilon)\eta_T k^2 + \alpha S k = 0. \quad (A6)$$

We eliminate ω to find critical dynamo number

$$\frac{|\alpha S k|}{(1 + \epsilon)\eta_T k^2} = \epsilon^{1/2} \eta_T k^2. \quad (A7)$$

We define the dynamo number

$$D \equiv |\alpha S k|/(\eta_T k^2)^2, \quad (A8)$$

and so the critical value is $D_{\text{crit}} = (1 + \epsilon)\epsilon^{1/2}$. The eigenfunction can be determined as

$$\overline{B}_x = \cos(kz - \omega t), \quad \overline{B}_y = Q \cos(kz - \omega t + \Delta\varphi), \quad (A9)$$

where

$$Q = \frac{S}{\eta_T k^2(1 + \epsilon)^{1/2}} = \frac{c}{\alpha} \sqrt{1 + \epsilon} \quad (A10)$$

is the toroidal to poloidal field ratio,

$$c = \frac{\omega}{k} = \frac{\alpha S}{\eta_T k^2(1 + \epsilon)} = \eta_T k \epsilon^{1/2} \text{sgn}(\alpha S) \quad (A11)$$

is the phase speed of the dynamo wave, and

$$\Delta\varphi = \text{atan}(\epsilon^{1/2}) \quad (A12)$$

is the phase shift. For $\epsilon = 1$ we have $\Delta\varphi = \pi/4$, whilst for $\epsilon = 0.1$ we have $\Delta\varphi \approx 0.1\pi$. For the two-dimensional model the phase shifts are larger: 0.33π for $\epsilon = 1$ and 0.30π for $\epsilon = 0.1$. This phase shift is related to φ_x and φ_y of Eq. (12) via

$$\Delta\varphi = \varphi_y - \varphi_x - \pi/2, \quad (A13)$$

so $\Delta\varphi = 0.3\pi$ corresponds to $\varphi_y - \varphi_x = 0.2\pi$, so the value of $|\langle \overline{\mathbf{J}} \cdot \overline{\mathbf{B}} \rangle|$ that enters in Sect. 4 is about 20% smaller than the maximum possible value.